Analysis of each branch current of serial solar cells by using an equivalent circuit model*

Yi Shi-Guang(易施光)[a], Zhang Wan-Hui(张万辉)[a)b)], Ai Bin(艾 斌)[a)], Song Jing-Wei(宋经纬)[a)], and Shen Hui(沈 辉)[a)†]

[a)] *Institute for Solar Energy Systems, State Key Laboratory of Optoelectronic Materials and Technologies, School of Physics and Engineering, Sun Yat-Sen University, Guangzhou* 510275, *China*

[b)] *Guangdong Testing Institute of Product Quality Supervision, Foshan* 528300, *China*

(Received 29 January 2013; revised manuscript received 23 May 2013; published online 20 December 2013)

In this paper, based on the equivalent single diode circuit model of the solar cell, an equivalent circuit diagram for two serial solar cells is drawn. Its equations of current and voltage are derived from Kirchhoff's current and voltage law. First, parameters are obtained from the *I*–*V* (current–voltage) curves for typical monocrystalline silicon solar cells (125 mm×125 mm). Then, by regarding photo-generated current, shunt resistance, serial resistance of the first solar cell, and resistance load as the variables. The properties of shunt currents (I_{sh1} and I_{sh2}), diode currents (I_{D1} and I_{D2}), and load current (I_L) for the whole two serial solar cells are numerically analyzed in these four cases for the first time, and the corresponding physical explanations are made. We find that these parameters have different influences on the internal currents of solar cells. Our results will provide a reference for developing higher efficiency solar cell module and contribute to the better understanding of the reason of efficiency loss of solar cell module.

Keywords: solar cell, equivalent circuit, current property

PACS: 88.40.–j, 88.40.fc, 88.40.jj, 88.40.H– **DOI:** 10.1088/1674-1056/23/2/028801

1. Introduction

With the continuous development of society and industry, demands for energy grow dramatically. However, as fossil energies (petroleum, coal, natural gas) are limited, stable and renewable energy sources are of great interest for human beings. Among those renewable energies, solar photovoltaic (PV) power is promising and various solar cell materials are being widely investigated.[1–9] However, the cost of PV devices will be higher for individual and mass applications if there is no government subsidy. Improving solar cell efficiency is one of ways to reduce the solar PV power cost. Hence, a detailed understanding of the PV device physics is necessary. A conventional silicon solar cell can be well described with a one-diode model or two-diode model. As far as the electrical research on solar cell is concerned, solar cell external current and output voltage have gained more attention than the internal current solar cells in series. Because the output voltage of one solar cell is usually lower than 0.8 V, the way of connecting several solar cells in series is generally adopted to increase the output voltage to meet the requirements of practical application. Consequently, it is important to investigate the current characteristics of serial solar cells in order to understand the working mechanism of a solar cell module and to increase its efficiency. Regarding photo-generated current, shunt resistance, serial resistance of the first solar cell, and resistance load as the variable quantities respectively, the properties of shunting currents (I_{sh1} and I_{sh2}), diode currents (I_{D1} and I_{D2}), and load current (I_L) for the two serial solar cells are analyzed with the relevant draws in these four cases for the first time in this paper. We find that these parameters exert different influences on the internal currents of solar cells. Our results will provide a reference for developing higher efficiency solar cell module and contribute to the better understanding of the internal reasons of efficiency loss of solar cell module.

This paper aims to extract the parameters of a typical silicon solar cell. First of all, the physical research model of solar cell is presented and the equations of current and voltage are derived from Kirchhoff's current and voltage law. Then, according to the measurement parameters of the current–voltage for the typical monocrystalline silicon solar cell (125 mm×125 mm), by using the numerical solution, regarding photo-generated current, shunt resistance, serial resistance of the first solar cell, and resistance load as the variable quantities respectively, the properties of shunting currents (I_{sh1} and I_{sh2}), diode currents (I_{D1} and I_{D2}), and loading current (I_L) for the two serial solar cells are analyzed with the relevant drawings in these four cases and the corresponding physical explanations are made. The conclusion of this paper are given at the end.

*Project supported by the National High Technology Research and Development Program of China (Grant No. 2012AA050302), the National Natural Science Foundation of China (Grant Nos. 61076059 and 51202301), and the Science & Technology Research Project of Guangdong Province, China (Grant No. 2011A032304001).

†Corresponding author. E-mail: shenhui1956@163.com

© 2014 Chinese Physical Society and IOP Publishing Ltd

2. Physical research model of solar cell

Photovoltaic energy conversion results from the product of electrical energy in the form of current and voltage from electromagnetic (i.e., light, including infrared, visible, and ultraviolet emission) energy. The successive four steps for this conversion are as follows: (i) a light absorption process which causes a transition of the absorber from a ground state to an excited one; (ii) the conversion of the excited state into (at least) a free negative and positive-charge carrier pair; (iii) a discriminating transport mechanism, which causes the free negative-charge carriers to move in the cathode direction and the free positive charge carriers to move in the opposite anode direction; and, (iv) a combination of negative charge with an arrived positive-charge carrier, thereby returning the absorber back to ground state.[10]

Solar cell operation is based on photovoltaic effect. Its essence is charge separation, and its driving force originates from the following four aspects: i) an electric field, which is the main driving force; ii) effective force fields (which change with position in affinities and band effective density of states), such as in a heterojunction solar cell and a dye-sensitized solar cell; iii) electron and hole diffusion difference (including carrier concentration gradient and carrier diffusion coefficient), such as Dember effect; and, iv) thermal diffusion resulting from temperature gradient. The driving force of formatting the built-in electric field is in the p–n junction form. A solar cell of built-in electric field driving force is actually a large area diode, which can produce a direct current by sunshine. According to the actual conditions and need of practical research, physical research models of solar cells have used a single diode equivalent circuit model,[11–18] double diode equivalent circuit model,[19–26] and double diode model of avalanche breakdown effect.[18,26–29] Since the double diode equivalent circuit model only shunts a diode which essentially produces dark current on the basis of single diode equivalent circuit model, the simulation result is more in line with actual measurement. Based on the double diode equivalent circuit model, the avalanche breakdown effect of double diode model shunts a reverse breakdown diode, which is equivalent to produce dark current in normal working condition, except its specific expression form, in which the breakdown diode is considered as a load under the condition of the high reverse bias. Consequently, in this paper the single diode equivalent circuit model is chosen, which is shown in Fig. 1.

According to Fig. 1 the mathematical expression of the dark current is as follows:

$$I_{\mathrm{D}} = I_{\mathrm{s}}\left[\exp\exp\left(\frac{qI_{\mathrm{sh}}R_{\mathrm{sh}}}{QkT}\right) - 1\right], \tag{1}$$

where q, k, Q, T, and I_{s} are the charge on the electron, namely 1.6022×10^{-19} C, Boltzmann constant, namely 1.3806×10^{-23} J/K, solar cell absolute temperature, the quality factor, and saturation current of the diode, respectively. According to the relevant theory of semiconductors, the diode saturation current is given by

$$I_{\mathrm{s}} = AqN_{\mathrm{C}}N_{\mathrm{V}}\left[\frac{1}{N_{\mathrm{A}}}\left(\frac{D_{\mathrm{n}}}{\tau_{\mathrm{n}}}\right)^{1/2} + \frac{1}{N_{\mathrm{D}}}\left(\frac{D_{\mathrm{p}}}{\tau_{\mathrm{p}}}\right)^{1/2}\right] \times \exp\left(-\frac{E_{\mathrm{g}}}{kT}\right), \tag{2}$$

where A, N_{C}, N_{V}, N_{A}, N_{D}, D_{p}, D_{n}, τ_{n}, τ_{p}, E_{g}, q, k, and T denote the area of p–n junction, effective state density of conduction band, effective state density of valence band, concentration of acceptor impurity, concentration of donor impurity, diffusion coefficient of electron, diffusion coefficient of hole, minority carrier lifetime of electron, minority carrier lifetime of hole, band gap of semiconductor material, charge on the electron, namely 1.6022×10^{-19} C, Boltzmann's constant, namely 1.3806×10^{-23} J/K, and solar cell absolute temperature, respectively.

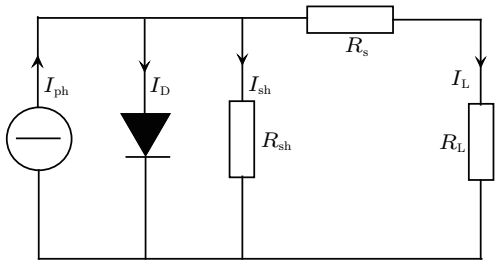


Fig. 1. Equivalent circuit model of the solar cell for the single diode, where I_{ph} is the current intensity of constant current source generated by the incident light, I_{sh} is the shunting current intensity of shunting resistance, which mainly consists of the cell edge leakage current and the recombination current of depletion region, R_{S} is the series resistance, which mainly includes positive metal electrode and semiconductor material contact resistance, semiconductor material body resistance, and electrode resistance, R_{L} is the loading resistance of external circuit, I_{L} is the current of external circuit, namely loading current, which can be measured, I_{D} is the dark current in the opposite direction of the photogenerated current, namely the diode leakage current, owing to the photogenerated electromotive force being p–n junction forward bias.

Since the output voltage of monolithic solar cell is very low, in application solar cells contain many solar cells in serial, namely solar cell module to meet practical needs. For example, nowadays, for manufacturing enterprises of crystalline silicon solar cells (including monocrystalline and polycrystalline silicon), the typical module is 60- or 72-cell solar cells of monocrystalline silicon or polycrystalline. However, the sixty or seventy-two solar cells are all in serial, and at present, the series standard of a single solar cell is that the parameters of the current and conversion efficiency of solar cells are consistent with each other or they are restricted within a range of permissible precision. Furthermore, the other parameters, such as series resistance, shunt resistance, and fill factor of solar cells, are hardly taken into account. Therefore, in research-

ing solar cell module, the single-solar-cell physical model reflects the comprehensive effect of solar cell module displays significant limitations. At this point, a multi-solar-cell physical model is appropriate; for example, the physical model of solar cell serial in this paper. In fact, the characterized parameters of solar cells do consist of a large number of factors, such as open-circuit voltage, maximum peak power voltage, short-circuit current, maximum peak power current, maximum peak power, fill factor, series resistance, shunting resistance, efficiency, cell temperature, intensity. The measurement parameters of the current–voltage for typical monocrystalline silicon solar cell 125 mm×125 mm are shown in Table 1.

However, with solar cells being considered as a constant current source, the effect of other parameters on the current of series solar cells should not be neglected, and it is necessary to analyze systematically and comprehensively the variation of solar cell series currents that originate from the variation of parameters of one series of solar cells. Especially, the analysis will play a part in theoretical guidance for the optimization of solar cell module and help to deeply understand the solar cell physical model. Then, on account of the equivalent circuit model of a solar cell single diode, the equivalent solar cell series circuit, which consists of two solar cells, will be discussed in detail. As shown in Fig. 2, according to Kirchhoff's law, equations can be derived as follows:

$$I_{D1} + I_{sh1} + I_L = I_{ph1}, \tag{3}$$

$$I_{D2} + I_{sh2} + I_L = I_{ph2}, \tag{4}$$

$$I_{D1} = I_{S1}\left[\exp\left(\frac{qI_{sh1}R_{sh1}}{Q_1 kT_1}\right) - 1\right], \tag{5}$$

$$I_{D2} = I_{S2}\left[\exp\left(\frac{qI_{sh2}R_{sh2}}{Q_2 kT_2}\right) - 1\right], \tag{6}$$

$$I_L\left(R_{S1} + R_{S2} + R_L\right) - I_{sh1}R_{sh1} - I_{sh2}R_{sh2} = 0. \tag{7}$$

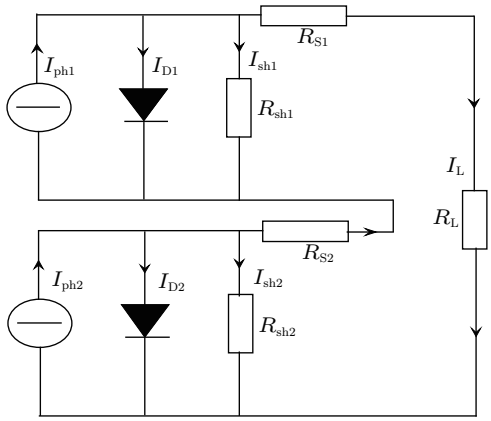


Fig. 2. Equivalent circuit model of the two solar cells in series.

In these equations, if I_{D1}, I_{D2}, I_{sh1}, I_{sh2}, and I_L are unknown variables, and the other ones are known, in principle, all the analytical expressions of the solutions of equations can be found for five equations with five unknown parameters. Owing to transcendental equations in Eqs. (3)–(7), the analytical solutions cannot be obtained under normal circumstances while the numerical solutions can be acquired with computer. Then, regarding the photo-generated current, shunt resistance, serial resistance of the first solar cell wafer, and loading resistance as the variables, the properties of shunting currents (I_{sh1} and I_{sh2}), diode currents (I_{D1} and I_{D2}), and loading current (I_L) for the two serial solar cells are discussed in detail for these four cases.

Table 1. Measurement parameters of the typical monocrystalline silicon solar cell 125 mm×125 mm.

Parameters	Cell 1	Cell 2	Cell 3	Cell 4	Cell 5	Cell 6	Unit
V_{oc}	0.626	0.623	0.624	0.624	0.626	0.626	V
V_{MPP}	0.522	0.521	0.522	0.521	0.522	0.524	V
I_{sc}	5.633	5.640	5.659	5.646	5.657	5.654	A
I_{MPP}	5.146	5.145	5.153	5.163	5.173	5.185	A
P_{MPP}	2.686	2.678	2.693	2.693	2.702	2.715	W
FF	76.17	76.20	76.25	76.42	76.29	76.71	%
R_s	8.772	8.547	8.374	8.537	8.797	8.459	mΩ
R_{sh}	14.162	14.809	14.964	14.192	14.893	14.325	Ω
Eff	17.35	17.30	17.39	17.39	17.45	17.54	%
Intensity	1198	1212	1200	1208	1186	1198	W/m^2
Temperature	24.6	24.6	24.6	24.6	24.6	24.6	°C

3. Numerical analyses and discussion

The following analyses are based on experiment data in Table 1. It is assumed that the photo-generated current, shunt resistance, serial resistance of the second solar cell wafer are all constant, and the corresponding parameters of the first solar cell wafer is varying.

3.1. Analysis of current properties with considering the photo-generated current as the variable

In order to discuss expediently, it is assumed that $I_{ph2} = 6.0$ A, $I_{S1} = I_{S2} = 1.0 \times 10^{-10}$ A, $R_{sh1} = R_{sh2} = 15\ \Omega$, $Q_1 = Q_2 = 1$, $T_1 = T_2 = 300$ K, $R_{S1} = R_{S2} = 8 \times 10^{-3}\ \Omega$, $R_L = 0.2\ \Omega$, $q = 1.6022 \times 10^{-19}$ C, $k = 1.3806 \times 10^{-23}$ J/K, and I_{ph1} is the dependent variable. As a result, the above Eqs. (3)–(7) are

written as follows:

$$I_{D1} + I_{sh1} + I_L = I_{ph1}, \tag{8}$$

$$I_{D2} + I_{sh2} + I_L = 6.0, \tag{9}$$

$$I_{D1} = 1.000 \times 10^{-10} \left[\exp\left(\frac{15 I_{sh1}}{0.026} \right) - 1 \right], \tag{10}$$

$$I_{D2} = 1.000 \times 10^{-10} \left[\exp\left(\frac{15 I_{sh2}}{0.026} \right) - 1 \right], \tag{11}$$

$$0.216 I_L - 15 I_{sh1} - 15 I_{sh2} = 0. \tag{12}$$

The numerical solutions of the above transcendental equation system are obtained and their properties are shown in detail in Fig. 3.

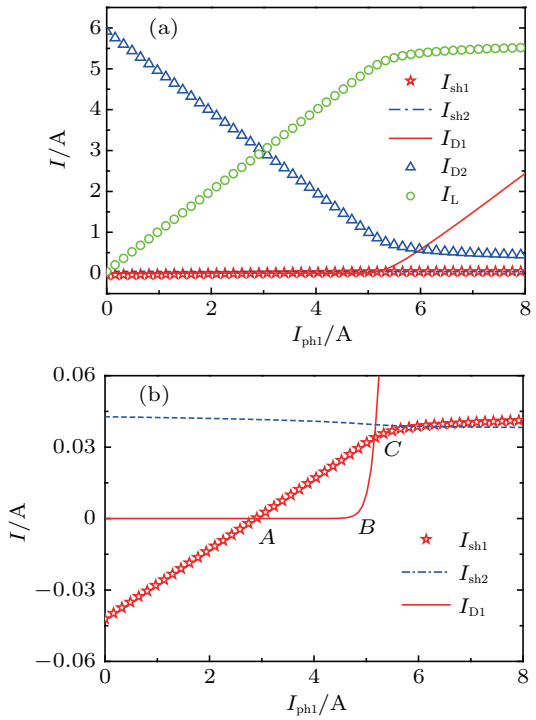


Fig. 3. (color online) Relations of the first solar cell and each branch current to photo-generated current: (a) the relations of I_{sh1}, I_{sh2}, I_{D1}, I_{D2}, and I_L to I_{ph1}; (b) the relations of I_{sh1}, I_{sh2}, and I_{D1} to I_{ph1} partially enlarged.

Figures 3(a) and 3(b), namely, the drawings of partial enlargement of I_{sh1}, I_{sh2}, I_{D1}, and I_{ph1}, show that I_{sh1} decreases when I_{ph1} increases from 0 to 3.0 A approximately, which is a negative value, namely being opposite to the direction of normal operating current; and that, with I_{ph1} further increasing from 3.0 A to 6.0 A, I_{sh1} increases with the positive value. In addition, I_{sh1} is slowly increasing when I_{ph1} is greater than 6.0 A. Meanwhile, I_{sh2} decreases slowly and monotonically when I_{ph1} increases, which is always a positive value ranging from 0.038 A to 0.043 A, approximately, namely the range of variation is very small.

Figures 3(a) and 3(b) show that I_{D1} decreases slowly as the photo-generated current I_{ph1} increases when I_{ph1} varies from 0 to 3.0 A, approximately, which is a negative value, namely the diode being reverse biased, and that, when I_{ph1} increases from 3.0 A to 5.5 A, I_{D1} increases slowly with the positive value, namely the diode being forward biased; I_{D1} rapidly increases when I_{ph1} is greater than 5.5 A. I_{D2} always decreases rapidly when I_{ph1} increases from 0 to 5.5 A, which is a positive value, namely the diode being forward biased; and I_{D2} declines moderately when I_{ph1} is greater than 5.5 A.

Figure 3(a) shows that I_L monotonically increases when I_{ph1} increases all the way, and rapidly increases when I_{ph1} is less than 5.5 A, and slowly increases when I_{ph1} is greater than 5.5 A.

In order to intuitively understand the reason why I_{sh1}, I_{sh2}, I_{D1}, I_{D2}, and I_L appear to regularly change when regarding I_{ph1} as the variable quantity. First of all, based on the relevant characteristics of the series circuit, R_{S1}, R_{S2}, and R_L will be replaced by equivalent resistance R_E, namely, $R_E = R_{S1} + R_{S2} + R_L$, then figure 2, namely, the equivalent circuit model for the two solar cells in series, may be simplified as shown in Fig. 4. Furthermore, on the basis of Kirchhoff's current law of node and diode nonlinear characteristics, combined with Fig. 4, it can qualitatively be explained that I_{sh1}, I_{sh2}, I_{D1}, I_{D2}, and I_L regularly vary with I_{ph1}.

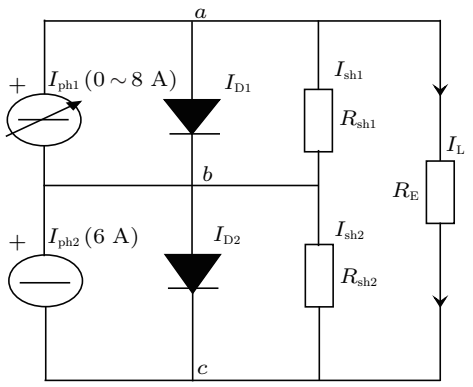


Fig. 4. Simplified circuit diagram of the equivalent circuit model of the two solar cells in series with regarding I_{ph1} as the variable quantity.

3.2. Analysis of current properties with considering the shunting resistance as the variable

For convenience, we choose that $I_{ph1} = I_{ph2} = 6.0$ A, $I_{S1} = I_{S2} = 1.0 \times 10^{-10}$ A, $R_{sh2} = 15\ \Omega$, $Q_1 = Q_2 = 1$, $T_1 = T_2 = 300$ K, $R_{S1} = R_{S2} = 8 \times 10^{-3}\ \Omega$, $R_L = 0.2\ \Omega$, $q = 1.6022 \times 10^{-19}$ C, $k = 1.3806 \times 10^{-23}$ J/K, and R_{sh1} is a dependent variable. Therefore, equations (3)–(7) will be written as follows:

$$I_{D1} + I_{sh1} + I_L = 6.0, \tag{13}$$

$$I_{D2} + I_{sh2} + I_L = 6.0, \tag{14}$$

$$I_{D1} = 1.0 \times 10^{-10} \left[\exp\left(\frac{R_{sh1} I_{sh1}}{0.026} \right) - 1 \right], \tag{15}$$

$$I_{D2} = 1.0 \times 10^{-10} \left[\exp\left(\frac{15 I_{sh2}}{0.026} \right) - 1 \right], \tag{16}$$

$$0.216I_{\rm L} - R_{\rm sh1}I_{\rm sh1} - 15I_{\rm sh2} = 0. \quad (17)$$

The numerical simulation results are shown in detail in Fig. 5.

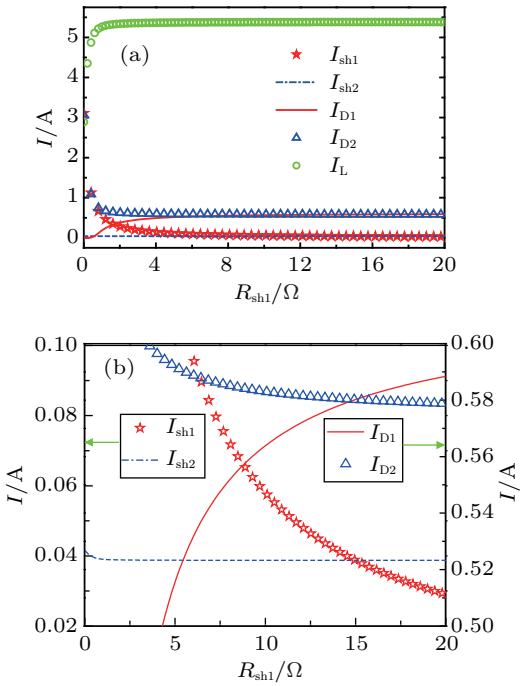


Fig. 5. (color online) Curves of the first solar cell and each branch current versus shunt resistance: (a) $I_{\rm sh1}$, $I_{\rm sh2}$, $I_{\rm D1}$, $I_{\rm D2}$, and $I_{\rm L}$ versus $R_{\rm sh1}$; (b) enlarged parts of curves of $I_{\rm sh1}$, $I_{\rm sh2}$, $I_{\rm D1}$, and $I_{\rm D2}$ versus $R_{\rm sh1}$.

Figures 5(a) and 5(b), namely, the drawings of partial enlargement of relevant curves, show that $I_{\rm sh1}$ and $I_{\rm sh2}$ decrease persistently and monotonically when $R_{\rm sh1}$ increases; and that $I_{\rm sh1}$ and $I_{\rm sh2}$ rapidly decrease when the interval of shunting resistance $R_{\rm sh1}$ range is approximately $0 \sim 1.0\ \Omega$; and that when $R_{\rm sh1}$ is greater than $1.0\ \Omega$, the shunting current $I_{\rm sh1}$ continues to reduce slowly, however, the shunting current $I_{\rm sh2}$ decrease more slowly than $I_{\rm sh1}$; and that when $R_{\rm sh1}$ is equal to $15\ \Omega$, approximately, the shunting currents $I_{\rm sh1}$ and $I_{\rm sh2}$ are the same. Obviously, when $R_{\rm sh1}$ is less than $1.0\ \Omega$, the shunting currents $I_{\rm sh1}$ and $I_{\rm sh2}$ will be greatly influenced.

Figures 5(a) and 5(b) manifest that the diode current $I_{\rm D1}$ increases monotonically as $R_{\rm sh1}$ increases, yet the diode current $I_{\rm D2}$ always decreases with the increase of $R_{\rm sh1}$, but the diode currents $I_{\rm D1}$ and $I_{\rm D2}$ are always positive, namely both of diodes are forward bias all the way; and that when the interval of $R_{\rm sh1}$ range is approximately $0 \sim 0.4\ \Omega$ the diode current $I_{\rm D1}$ evenly increases, when the interval of $R_{\rm sh1}$ range is approximately $0.4\ \Omega \sim 5.0\ \Omega$, $I_{\rm D1}$ rapidly increases, for the case that $R_{\rm sh1}$ is greater than $5.0\ \Omega$, $I_{\rm D1}$ slowly increases again; while the interval of $R_{\rm sh1}$ range is $0 \sim 2.0\ \Omega$, approximately, $I_{\rm D2}$ sharply decreases; in contrast, larger value of $R_{\rm sh1}$ will lead to slowly reducing $I_{\rm D2}$; in addition, when $R_{\rm sh1}$ is equal to $15\ \Omega$, approximately, the values of $I_{\rm D1}$ and $I_{\rm D2}$ are the same. It is obvious that $R_{\rm sh1}$, whose value is less than $5.0\ \Omega$, will have a greater influence on $I_{\rm D1}$ and $I_{\rm D2}$.

Figure 5(a) indicates that $I_{\rm L}$ increases monotonically as $R_{\rm sh1}$ increases, and that when the interval of $R_{\rm sh1}$ range is approximately $0 \sim 1.0\ \Omega$, $I_{\rm L}$ drastically increases, when it is greater than $1.0\ \Omega$ the loading current $I_{\rm L}$ slowly increases. It is clear that when $R_{\rm sh1}$ is less than $1.0\ \Omega$, $I_{\rm L}$ is sensitive to the variation of $R_{\rm sh1}$.

In order to intuitively understand the reason why $I_{\rm sh1}$, $I_{\rm sh2}$, $I_{\rm D1}$, $I_{\rm D2}$, and $I_{\rm L}$ appear to regularly change when regarding $R_{\rm sh1}$ as the variable quantity, first of all, based on the relevant characteristics of the series circuit and properties of constant current source, figure 2 may be simplified into Fig. 6. Furthermore, on the basis of Kirchhoff's current law of node and diode nonlinear characteristics, combined with Fig. 6, it can qualitatively be explained that $I_{\rm sh1}$, $I_{\rm sh2}$, $I_{\rm D1}$, $I_{\rm D2}$, and $I_{\rm L}$ regularly vary with $R_{\rm sh1}$.

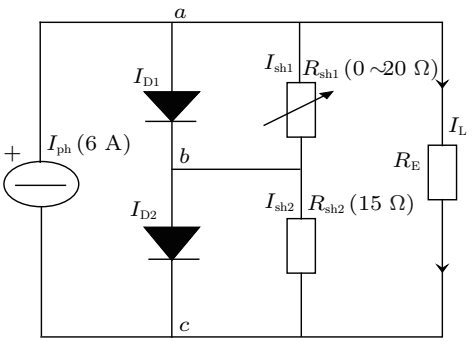


Fig. 6. Simplified circuit diagram of the equivalent circuit model for the two solar cells in series with regarding $R_{\rm sh1}$ as the variable quantity.

In conclusion, in order to ensure that each current of mutual serial cells can be affected least, the shunt resistance should be as large as possible.

3.3. Analysis of current properties with considering the serial resistance as the variable

In order to discuss expediently, it is assumed that $I_{\rm ph1} = I_{\rm ph2} = 6.0$ A, $I_{\rm S1} = I_{\rm S2} = 10^{-10}$ A, $R_{\rm sh1} = R_{\rm sh2} = 15\ \Omega$, $Q_1 = Q_2 = 1$, $T_1 = T_2 = 300$ K, $R_{\rm S2} = 8 \times 10^{-3}\ \Omega$, $R_{\rm L} = 0.2\ \Omega$, $q = 1.6022 \times 10^{-19}$ C, $k = 1.3806 \times 10^{-23}$ J/K, and $R_{\rm S1}$ is a dependent variable. Consequently, the above equations (3)–(7) will be written as follows:

$$I_{\rm D1} + I_{\rm sh1} + I_{\rm L} = 6.0, \quad (18)$$

$$I_{\rm D2} + I_{\rm sh2} + I_{\rm L} = 6.0, \quad (19)$$

$$I_{\rm D1} = 1.0 \times 10^{-10}\left[\exp\left(\frac{15I_{\rm sh1}}{0.026}\right) - 1\right], \quad (20)$$

$$I_{\rm D2} = 1.0 \times 10^{-10}\left[\exp\left(\frac{15I_{\rm sh2}}{0.026}\right) - 1\right], \quad (21)$$

$$(0.208 + R_{\rm S1})I_{\rm L} - 15I_{\rm sh1} - 15I_{\rm sh2} = 0. \quad (22)$$

The numerical solutions of the above transcendental equation system are shown in Fig. 7.

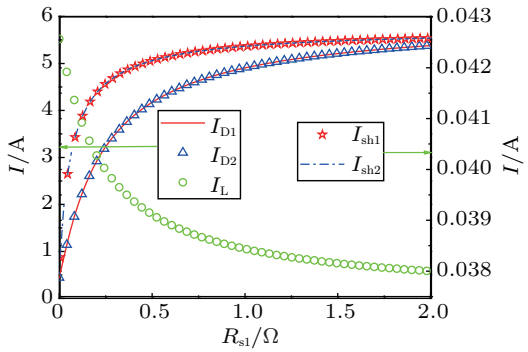


Fig. 7. (color online) relations of the first solar cell and each branch current to series resistance: the relations between I_{sh1}, I_{sh2}, I_{D1}, I_{D2}, I_L, and R_{S1}.

Figure 7 reveals that I_{sh1} and I_{sh2} increase monotonically when R_{S1} increases; and that I_{sh1} and I_{sh2} rapidly increases when the interval of R_{S1} range is approximately $0 \sim 0.1\ \Omega$; and that when R_{S1} is greater than $0.1\ \Omega$, the shunting currents I_{sh1} and I_{sh2} continue to slowly increase. Obviously, when R_{S1} is less than $0.1\ \Omega$, I_{sh1} and I_{sh2} are vulnerable to the change of R_{S1}.

Figure 7 shows that I_{D1} and I_{D2} display similar variable trends to the I_{sh1} and I_{sh2} do when R_{S1} increases, furthermore, the diode currents I_{D1} and I_{D2} are always positive, namely both of diodes are forward bias all the way; and that I_{D1} and I_{D2} rapidly increase when the interval of serial resistance R_{S1} range is approximately $0 \sim 0.5\ \Omega$; and that when R_{S1} is greater than $0.5\ \Omega$, the diode currents I_{D1} and I_{D2} slowly increase. It becomes obvious that when R_{S1} is less than $0.5\ \Omega$, it will play an important role for I_{D1} and I_{D2}.

According to Fig. 7, I_L decreases monotonically with the increasing of R_{sh1}. What is more, I_L declines sharply, except in the case where the value of R_{S1} is larger than $0.5\ \Omega$, approximately.

In order to intuitively understand the reason why I_{sh1}, I_{sh2}, I_{D1}, I_{D2}, and I_L appear to regularly change when regarding R_{S1} as the variable quantity, first of all, based on the relevant characteristics of the series circuit, properties of constant current source and the symmetry of chosen parameters, figure 2 may be simplified into Fig. 8. Furthermore, on the basis of

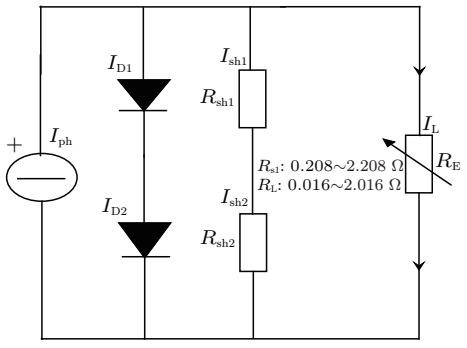


Fig. 8. Simplified circuit diagram of the equivalent circuit model for the two solar cells in series with regarding R_{S1} and R_L as the variable quantities.

Kirchhoff's current law of node and diode nonlinear characteristics, combined with Fig. 8, it can qualitatively be explained that I_{sh1}, I_{sh2}, I_{D1}, I_{D2}, and I_L regularly vary with R_{S1}.

The above analysis demonstrates that, if the photo-generated currents, shunting resistances and loading resistance are invariant, then the less serial resistances will contribute to less I_{sh1}, I_{sh2}, I_{D1}, I_{D2}, and larger I_L.

3.4. Analysis of current properties with considering the loading resistance as the variable

For convenience, it is assumed that $I_{ph1} = I_{ph2} = 6.0$ A, $I_{S1} = I_{S2} = 10^{-10}$ A, $R_{sh1} = R_{sh2} = 15\ \Omega$, $Q_1 = Q_2 = 1$, $T_1 = T_2 = 300$ K, $R_{S1} = R_{S2} = 8 \times 10^{-3}\ \Omega$, $q = 1.6022 \times 10^{-19}$ C, $k = 1.3806 \times 10^{-23}$ J/K, and R_L is a dependent variable. Thus, the above equations (3)–(7) will be written as follows:

$$I_{D1} + I_{sh1} + I_L = 6.0, \tag{23}$$

$$I_{D2} + I_{sh2} + I_L = 6.0, \tag{24}$$

$$I_{D1} = 1.0 \times 10^{-10}\left[\exp\left(\frac{15I_{sh1}}{0.026}\right) - 1\right], \tag{25}$$

$$I_{D2} = 1.0 \times 10^{-10}\left[\exp\left(\frac{15I_{sh2}}{0.026}\right) - 1\right], \tag{26}$$

$$(0.016 + R_L)\, I_L - 15I_{sh1} - 15I_{sh2} = 0. \tag{27}$$

The numerical solutions of Eqs. (22)–(27) are shown in detail in Fig. 9.

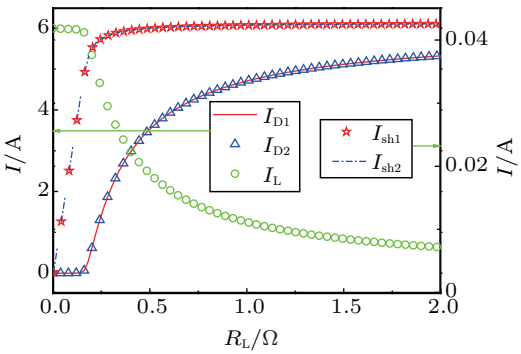


Fig. 9. (color online) Relations of each branch current to series load resistance: the relations between I_{sh1}, I_{sh2}, I_{D1}, I_{D2}, I_L, and R_L.

Figure 9 denotes that the values of I_{sh1} and I_{sh2} rise monotonically with the variance of R_L; I_{sh1} and I_{sh2} go up rapidly when R_L changes approximately in a range of $0 \sim 0.25\ \Omega$; and when R_L is greater than $0.25\ \Omega$, I_{sh1} and I_{sh2} vary evenly. This implies that R_L exerts a greater influence on I_{sh1} and I_{sh2} when it is between 0 to $0.25\ \Omega$.

Figure 9 indicates that I_{D1} and I_{D2} increase monotonically as R_L increases, furthermore, I_{D1} and I_{D2} are always positive, namely both of the diodes are forward bias all the way; and that I_{D1} and I_{D2} slowly increase when R_L is approximately $0 \sim 0.15\ \Omega$; and that I_{D1} and I_{D2} rapidly increase when R_L is approximately $0.15\ \Omega \sim 1.0\ \Omega$; and that when R_L is greater than $1.0\ \Omega$, I_{D1} and I_{D2} slowly increase. Obviously, I_{D1} and

I_{D2} are sensitive to the change of R_L as long as its value is less than 1.0 Ω.

Figure 9 shows that I_L decreases monotonically as R_L increases; and that I_L slowly decreases when the interval of R_L range is approximately $0 \sim 0.15$ Ω; and that I_L rapidly decreases when the interval of R_L range is approximately 0.15 Ω∼1.0 Ω; and that I_L slightly decreases when R_L is greater than 1.0 Ω.

In order to intuitively understand the reason why I_{sh1}, I_{sh2}, I_{D1}, I_{D2}, and I_L appear to regularly change when regarding R_L as the variable quantity, first of all, based on the relevant characteristics of the series circuit, properties of constant current source and the symmetry of chosen parameters, figure 2 may be simplified into Fig. 8, which is the same as that when R_{S1} is regarded as the variable quantity, but the starting value of R_E when R_L is regarded as the variable quantity is much less than that when R_{S1} is regarded as the variable quantity. Furthermore, on the basis of Kirchhoff's current law of node and diode nonlinear characteristics, combined with Fig. 8, it can qualitatively be explained that I_{sh1}, I_{sh2}, I_{D1}, I_{D2}, and I_L regularly vary with R_L.

The above analyses show that if the photo-generated currents, shunting resistances, and serial resistance are fixed, less loading resistances will result in less I_{sh1} and I_{sh2} and larger I_L.

4. Conclusion

In this paper, based on the equivalent circuit model of solar cell for the single diode, we utilize Kirchhoff's current and voltage law to depict the equivalent circuit diagram of the two solar cell wafers in series. According to the relevant parameters of current–voltage for the typical monocrystalline silicon solar cell (125 mm×125 mm), the numerical simulation is employed to investigate the properties of I_{sh1}, I_{sh2}, I_{D1}, I_{D2}, and I_L when we set the I_{ph1}, R_{S1}, R_{sh1}, and R_L as the variable and their corresponding physical explanations are made.

In addition, the results we acquired indicate that I_{ph}, R_S, R_{sh}, and R_L have significant effects on current and power output of the serial solar cells. As a result, in order to ensure best conversion efficiency and power output of the serial solar cells when the solar cells wafers are cascaded, various parameters should be comprehensively taken into account. Furthermore, the numerical simulation result in this paper should not be restricted to such a typical monocrystalline silicon solar cell (125 mm×125 mm) alone, and it should also become suitable for the other types of solar cell with different sizes. Thus, this research has a certain universality and provides significant theoretical guidance for the development of solar photovoltaic technology.

Acknowledgment

We give the most sincere thanks to Drs. X C Zhang, W S Li, and F P Lu for their useful discussion.

References

[1] Li P J, Chen K, Chen Y F, Wang Z G, Hao X, Liu J B, He J R and Zhang W L 2012 *Chin. Phys. B* **21** 118101
[2] Chen W B, Xu Z X, Li K, Chui Stephen S Y, Roy V A L, Lai P T and Che C M 2012 *Chin. Phys. B* **21** 078401
[3] Zhang X D, Zheng X X, Xu S Z, Lin Q, Wei C C, Sun J, Geng X H and Zhao Y 2011 *Chin. Phys.* B **20** 108801
[4] Zhang X B, Wang X L, Xiao H L, Yang C B, Hou Q F, Yin H B, Chen H and Wang Z G 2011 *Chin. Phys.* B **20** 028402
[5] Chen D S, Yang J, Xu F, Zhou P H, Du H W, Shi J W, Yu Z S, Zhang Y H, Brian B and Ma Z Q 2013 *Chin. Phys. B* **22** 018801
[6] Zhou N, Zhang Y D, Sun H C , Qin D, Luo Y H, Li D M and Meng Q B 2011 *Physics* **40** 72 (in Chinese)
[7] Wang D, Chu Z Z, Zhang C and Zou D C 2011 *Physics* **40** 241 (in Chinese)
[8] Zhao J and Zeng Y P. 2011 *Physics* **40** 233 (in Chinese)
[9] Qu B, Zhang S Y, Xie X, Chen Z J, Xiao L X, Gong Q H, Li F S and Guo T L 2011 *Physics* **40** 223 (in Chinese)
[10] Fonash S J 2010 *Solar Cell Device Physics*, 2nd edn. (Waltham: Academic Press) pp. 1–8
[11] Shen H and Zeng Z Q 2009 *Solar Photovoltaic Power Generation Technology* (Beijing: Chemical Industry Press) pp. 34–36 (in Chinese)
[12] Zhang Z, Shen H, Zhu J J and Cai R X 2008 *Proceeding of* 10*th China Solar Photovoltaic Conference*, September 19–22, 2008, Changzhou, China, p. 964 (in Chinese)
[13] Bishop J W 1988 *Solar Energy* **25** 73
[14] Aberle A G, Wenham S R and Green M A 1993 *Proceedings of the* 23*rd IEEE Photovoltaic Specialists Conference*, May 10–14, 1993, Louisvills, USA, p. 133
[15] Aberle A G, Wenham S R and Green M A 1994 *Prog. Photovolt: Res. Appl.* **2** 3
[16] Aberle A G, Robinson S J, Wang A H, Zhao J H, Wenham S R and Green M A 1993 *Prog. Photovolt: Res. Appl.* **1** 133
[17] You H L and Zhang C F 2009 *Chin. Phys. B* **18** 2096
[18] Yong S K, Sung-Mo K, Bruce J and Roland W 2013 *Solar Energy Materials and Solar Cells* **115** 21
[19] Ding J L, Cheng X F, Zhai Z T, Zha J and Mao M Q 2007 *Acta Energiae Solaris Sinica* **28** 1312 (in Chinese)
[20] Badescu V 2003 *Energy* **28** 1165
[21] Hamdy M A and Call R L 1987 *Solar Cells* **20** 119
[22] Handy R J 1967 *Solid-State Electronics* **10** 765
[23] Mette A 2007 "New Concepts for Front Side Metallization of Industrial Silicon Solar Cells", Ph. D. Thesis (Freiburg im Breisgau: Fraunhofer-Institut fur Solare Energies Systeme)
[24] Hilali M M 2005 "Understanding and Development of Manufacturable Screen Printed Contacts on High Sheet-Resistance Emitters for Low-Cost Silicon Solar Cells", Ph. D. Thesis (Atlanta Botanical: Georgia Institute of Technology)
[25] Wang,M D, Zheng S Z, Wan X, Su Y R, Ke N, Zhao N, Wong K Y and Xu J B 2013 *Solar Energy Materials and Solar Cells* **108** 17
[26] Bernardez L D and Buitrango H R 2006 *Progress in Photovoltaics: Research and Applications* **14** 321
[27] Quaschning V and Hanitsch R 1996 *Solar Energy* **56** 513
[28] Liu B Y, Duan S X and Kang Y 2008 *Acta Energiae Solaris Sinica* **29** 188 (in Chinese)
[29] Li G L, Li M, Wang L L, Xiang M, Huang B, Zheng S F, Wei S X and Wang Y F 2011 *Acta Opt. Sin.* **30** 0125001 (in Chinese)